Proceedings of the Korean Nuclear Society Autumn Meeting
YongPyung, Korea, October 2003

Characteristics of Strain Aging Phenomena in Nuclear Structural Grade Low Alloyed Carbon Steel with Heat Treatment

J.S. Lee, I.S. Kim, J.K. Park

Korea Advanced Institute of Science and Technology
373-1, Gusong-dong, Yusong-gu, Daejeon 305-701, South Korea

Abstract

Intercritical annealing treatment in two-phase ($\alpha+\gamma$) region was performed to the SA106 Gr.C piping steel to reduce detrimental effects on the mechanical properties resulted from the strain aging phenomena. Tensile tests were carried out under various temperatures and strain rates, and yield point return technique was conducted to measure the relative interstitial solute content. The manifestations of dynamic stain aging were still observed in the tensile and J-R tests of the annealed specimens. However, the ductility loss was smaller than that in the as-received. Further, compared to the as-received condition, the temperature of minimum fracture properties, such as J-R, J_i and dJ/da, was shifted to higher temperature with the heat treatment. The activation energy of interstitial carbon atoms determined by Hartley analysis method and Arrhenius equation was ranged from 117.4 to 125.54 kJ/mol, which was larger than the conventional interstitial bulk diffusion. It seems that those reduced strain aging effects were induced by a reduction of interstitial carbon content in a ferrite matrix with the heat treatment.

INTRODUCTION

The SA106 Gr.C piping steel, which was selected for Korea Next Generation Reactor (KNGR) and already used in PWR main steam line, and other similar grade carbon steels showed a substantial reduction in toughness due to dynamic strain aging (DSA) at the reactor operating temperature [1, 2], which caused some detrimental effects to the structural integrity.

Strain aging in ferritic steels is defined as the changes in mechanical and physical properties of a metal that occur by the interstitial solute atoms and dislocations as a function of time and temperature. When the property changes occur after plastic deformation, the process is called static strain aging (SSA). However, when they are concurrent with plastic deformation, the process is called dynamic strain aging. DSA in ferritic steels is usually accompanied by serrated stress-strain curves and increased rates of strain hardening.

Since strain aging entails interaction between mobile interstitial solutes and dislocations, the solute concentration in ferrite matrix influence the degree of strain aging characteristics. Therefore, to relieve deleterious DSA effects it was suggested that the interstitial solute content be reduced. However, the amount of dissolved nitrogen and carbon for strain aging is extremely small, as demonstrated by Wilson and Russell [3], the concentration of interstitial solute atoms in solid solution must be reduced to about 0.0001% or less to eliminate the effects of strain aging, complete elimination of strain aging is difficult. Yet, it is possible to control degree of strain aging by adding alloying elements or by heat treatment. Owing to the relatively high carbon content in the ferrite matrix of SA106 Gr.C piping steel, which was processed by normal air-cooling after hot extrusion, it was severely affected by DSA. Therefore, to take cleaner ferrite (low carbon content) matrix, an intercritical annealing treatment, performed at the $\alpha+\gamma$ region, was introduced.

The aim of the present work is to reduce DSA susceptibility through additional heat treatment and to give sufficient safety margins of structural integrity.

EXPERIMENTAL

Material and the heat treatment

The SA106 Gr.C carbon steel used in this work was received from Hanjung Co. Ltd, which was the archive material of main steam line piping of Young-Gwang Unit 3&4. It was fabricated by normal air-cooling after hot drawing. The chemical analyses are given in Table 1. The microstructure was a typical ferrite-pearlite band structure with average grain size of 20 micrometer. As-received SA106 Gr.C was homogenized in the austenite range at 950℃ for 1hr in a vacuum furnace and furnace cooled. Then they were annealed in the intercritical two-phase, ferrite plus austenite phase, field at 760℃. After the annealing for *40 min*, the specimens were subjected to

furnace cooling.

Mechanical Testing and Metallography

The tensile specimens were machined to *8 mm* diameter and *40mm* gage length such that their tensile axis was parallel to pipe axis. Tensile tests were carried out at various temperatures, from RT to 350°C, and at a strain rates of 1.39×10^{-4} to 1.39×10^{-2}. Specimen temperature was measured by spot-welded thermocouple to the upper and lower parts in the specimen, and strain was measured with 0.1inch extensometer. 1T compact tension (CT) specimens were machined according to ASTM E-1820. Nital and stained boiling alkaline chromate solution (*8g* CrO_3 *+ 40g NaOH + 72 ml pure water*) revealed the microstructures composed of a pearlite and both kinds of ferrite, retained (old) and transformed (new).

Measurement of Aging Index and J-R tests

Tensile specimens of *20mm* gage length and *4mm* diameter were prepared from the as-received and intercritical heat-treated SA106 Gr.C piping steel, respectively, and pre-strained at about *7%* at a strain rate of 2×10^{-3}. After straining, the tensile specimens were aged at temperatures in the range of 132 ~ 170°C for times up to *15,930 min* in a dry oven with a temperature control of *±1 °C*, then water quenched and re-tested in tension until fracture. The increase in yield stress $\Delta\sigma$ due to aging is defined as $(\sigma_y - \sigma_f)$, the difference between σ_y, the yield stress after aging and σ_f, the flow stress at the end of straining. Aging index is defined as $\Delta\sigma/\overline{\sigma}$, where $\overline{\sigma}$ is $(\sigma_y + \sigma_f)/2$.

According to the ASTM E1820-96, fatigue pre-cracking in 1T CT specimens was performed by Instron 8501 machine in a range of a/W=0.55~0.58. J-R tests were carried out at various temperatures, from RT to 350°C. Load-line displacement rate was 0.4 and 4.0 mm/min and crack growth was measured a DCPD (direct current potential drop) method. The crack initiation toughness, Ji, was defined as the values of the J-integral at the crack initiation point obtained from DCPD method. The crack growth resistance, dJ/da, was determined by the first order linear fit in J-R curve in which crack increment (Δa) ranged from 0.5 to 2.5 mm.

RESULTS AND DISCUSSION

Microstructures

Fig.1 illustrates the optical microstructures of the as received and the heat-treated condition. In Fig.1 (a) shows typical ferrite-pearlite banding structure. It was reported that banding is primary due to microsegregation of manganese, non-metallic inclusion and cooling rates [4]. After the intercritical annealing treatment the microstructure of SA106 Gr.C was changed like a Fig1. (b). It shows a rather dispersed and discontinues pearlite band layers are randomly distributed.

Owing to the intercritical annealing treatment we could obtain both kinds of ferrite. The optical micrographs are shown in Fig.2. To distinguish between retained and transformed ferrite, boiling alkaline chromate solution stained the heat-treated specimen. The pearlite was stained black and the ferrite, which was co-existed with the austenite, was stained gray. This ferrite was called retained (old) ferrite. The ferrite formed at cooling from the intercritical annealing temperature, called transformed (new), stained white.

Tensile Tests

The dependence of stress-strain curves on the test temperature at a strain rate of 1.39×10^{-3} is shown in Fig.3. Typical Luder's strain occurred at lower temperature and disappeared with increasing temperature. From the results of tensile tests the serrated flow behavior has been observed at a certain combination of temperature and strain rate, but the stress amplitude was not severe compared to other similar grade carbon steels [1]. This reduced sensitivity on DSA seems to be related to high manganese content. It is generally known that the larger amount of manganese content could relieve DSA sensitivity and shift DSA region to the higher temperature [5].

To investigate the effects of intercritical annealing treatment, reduction of area was measured on the as received and the heat-treated specimen. According to Fig.3 (b), loss of reduction in area induced by DSA was clearly observed at both cases. However, heat-treated specimens exhibited relatively small amount of ductility loss compared to as received. It could be explained with the fact that soft retained ferrite and dispersed pearlite band formed by the intercritical annealing gave higher ductility than that of as received condition. From the Fe-C phase diagram, it is evident that

the carbon content in solid solution in the retained ferrite, which was formed at region, may be lower than that in the transformed [6].

Characteristics of Strain Aging

Aging phenomena

Fig. 4(a) describes the aging in the pre-strained specimens at 170℃ with respect to changes in yield stress. The typical distinct features are as follow. i) an increase in yield stress during aging but sharp upper yield point was not observed at this experiment, ii) a return of yield point elongation (Luder's strain) and an increase in this strain with increasing aging time. In Fig. 4(b), the aging index, the fractional increase in yield-stress, $\Delta\sigma/\overline{\sigma}$, was plotted against the aging time for the as received and heat-treated specimen, respectively. As time goes on up to 6×10^5 sec the aging index increased and remained constant or decreased slightly with further aging. This increment of aging index was attributed to the formation of Cottrell atmospheres by long-range diffusion of interstitial solutes outside the strained region. After completion of Cottrell atmospheres, the solutes formed cluster or precipitate, which resulted in precipitation hardening.

In Fig. 4(b), it was observed that longer aging times are required to achieve the same aging index after the intercritical annealing treatment. It is believed that this behavior is a result of the reduction in the concentrations of solute carbon in the matrix. Since there is less carbon to pin dislocations in heat-treated material, the carbon atoms must diffuse longer distances for pinning.

Kinetics of Strain Aging

The initial stage of strain aging process is attributed to the relationship of interstitials and dislocation. In Fig. 5 (a), the initial stage of $\Delta\sigma/\overline{\sigma}$ versus $t^{2/3}$ yielded a linear relationship as coincidence with the previous work [7]. To combine single expression, $\Delta\sigma/\overline{\sigma}$, aging time and temperature, Hartley [8] modified the Cottrell-Bilby $t^{2/3}$ relationship as follows:

$$\Delta\sigma/\overline{\sigma} = K_1 + K_2(Dt/T_a)^{2/3} \qquad (1)$$

where K_1 and K_2 are constant , t is the aging time, T_a is the aging temperature and D is the diffusion coefficient of pinning element, given by $D = D_0 \exp(-Q/RT_a)$, where Q is the activation energy. In Fig. 5 (b) logarithmic $STa^{2/3}$ *versus 1/T* is shown for the initial stage of strain aging, where $slope(S) = K_2(D/T_a)^{2/3}$. From the above equation, we could obtain the activation energy Q in the initial stage of strain aging. In case of as received material it was 121.65 kJ/mol and in case of heat-treated it was 117.4 kJ/mol. These activation energies are good agreement with the result of Kim and Kim (124.3 kJ/mol)[2]. But, the value of activation energy in this result was higher than that in the bulk diffusion of carbon or nitrogen in α-iron (62.8~83.7 kJ/mol). It was resulted from the fact that manganese by forming Mn-C pairs reduces the mobility of the carbon atoms in ferrite matrix [9]. To check the method used by Hartley, the activation energy was also determined by Arrhenius equation. Using this method, activation energy of 125.54 and 124.9 kJ/mol were computed, which is good agreement with the value determined by Hartley analysis method.

Characteristics of Fracture Properties

The dependence of the fracture resistance on temperature and loading rate was apparent, irrespective of heat treatment. As the temperature increased from room temperature, the J-R curves exhibited lower values until a critical temperature reached and increased again at higher temperatures. The critical temperature at which the J-R curve attained a minimum, were shifted to higher temperature with faster loading rate. The variation of Ji and dJ/da with temperature for each loading rate is given in Fig. 6, 7. The trend of variation in Ji and dJ/da with temperature and loading rate was similar with J-R curves. In as-received specimen, the minimum point appeared at temperature of 200-250 and 250-296℃ for load-line displacement rates of 0.4 and 4.0 mm/min, respectively. The minimum point, however, was shifted to higher temperature with the heat treatment. It appeared at temperature of 289 and above350 ℃ for load-line displacement rates of 0.4 and 4.0 mm/min, respectively.

CONCLUSION

The effects of intercritical annealing treatment on the static and dynamic strain aging

characteristics of SA106 Gr.C piping steel were investigated.

1. Dynamic strain aging phenomena in the heat-treated SA106 Gr.C were also observed in tensile properties. However, the magnitude of serration and strength increased by DSA were relatively small compare to similar grade carbon steel. Also, ductility loss caused by DSA was somewhat relieved with the heat treatment.
2. It was observed that longer aging times are required to achieve the same aging index after the intercritical annealing treatment. It is believed that this behavior is a result of the reduction in the concentrations of solute carbon in the ferrite matrix.
3. The activation energy for segregation of interstitial carbon to the dislocation was 117.4~125.54 kJ/mol, which is rather higher than that in the bulk diffusion of carbon in α-iron.
4. Compared to the as-received condition, the temperature of minimum fracture properties, J-R, Ji and dJ/da, was shifted to higher temperature with the heat treatment. It seems that the reduced strain aging phenomena were induced by cleaner (low carbon content) retained ferrite with the heat treatment.

ACKNOWLEDGMENT

This work has been supported by EESRI (99-지-05), which is funded by MOCIE(Ministry of commerce, industry and energy)

REFERENCES

1. D. O. Haarris, E. Y. Lim and D.D. Dedhia, *NUREC/CR-2189*, **5**, Nuclear Regulatory Commission (1981).
2. J. W. Kim and I. S. Kim, *Nuclear Engineering and Design*, **172**, pp. 49~59 (1997).
3. D. V. Wilson and B. Russell, *Acta Metallurgica*, **8**, pp.468~479 (1960).
4. W. C. Leslie, *The Physical Metallurgy of Steels*, pp.172, McGraw –Hill (1982).
5. C. C. Li and W. C. Leslie, *Metallurgical Transactions A*, **9A**, pp.1765~1775 (1978).
6. J.J. Yi and I. S. Kim, *Scripta Metallurgica*, **17**, pp. 299~302 (1983).
7. H.E. Rosinger, *Metal Science*, **9**, pp. 1~7 (1975).

8. S. Hartley, *Acta Metallurgica*, **14**, pp. 1237~1246 (1966).
9. J. Gouzou, J. Wegria and L. Habraken, *Metallurgical Reports*, No. 33, CRM, Liege, pp. 65 (1972).

Table 1. Chemical Composition of SA106 Gr.C (w/o)

C	Mn	P	S	Si	Ni	Cr	Mo	V	Al	Cu	Hppm
0.19	1.22	0.009	0.007	0.27	0.11	0.05	0.03	0.004	0.029	0.13	1.6

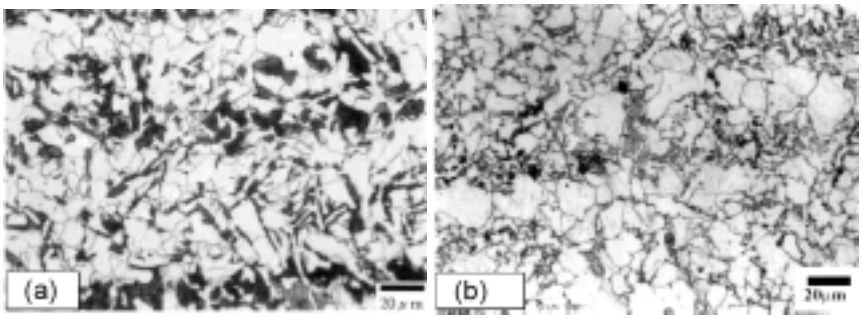

Fig. 1. The microstructures of SA106 Gr.C. (a) as received, (b) heat-treated, 2% nital etched

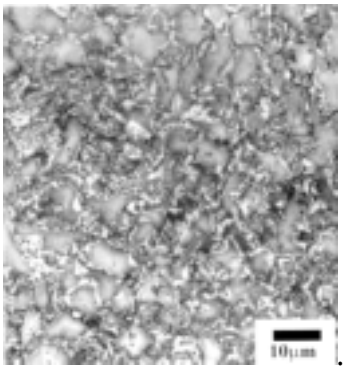

Fig. 2. The optical micrograph of heat-treated SA106 Gr.C. The gray areas are retained ferrite, the white areas are transformed and black areas are pearlite, boiling alkaline chromate solution stained

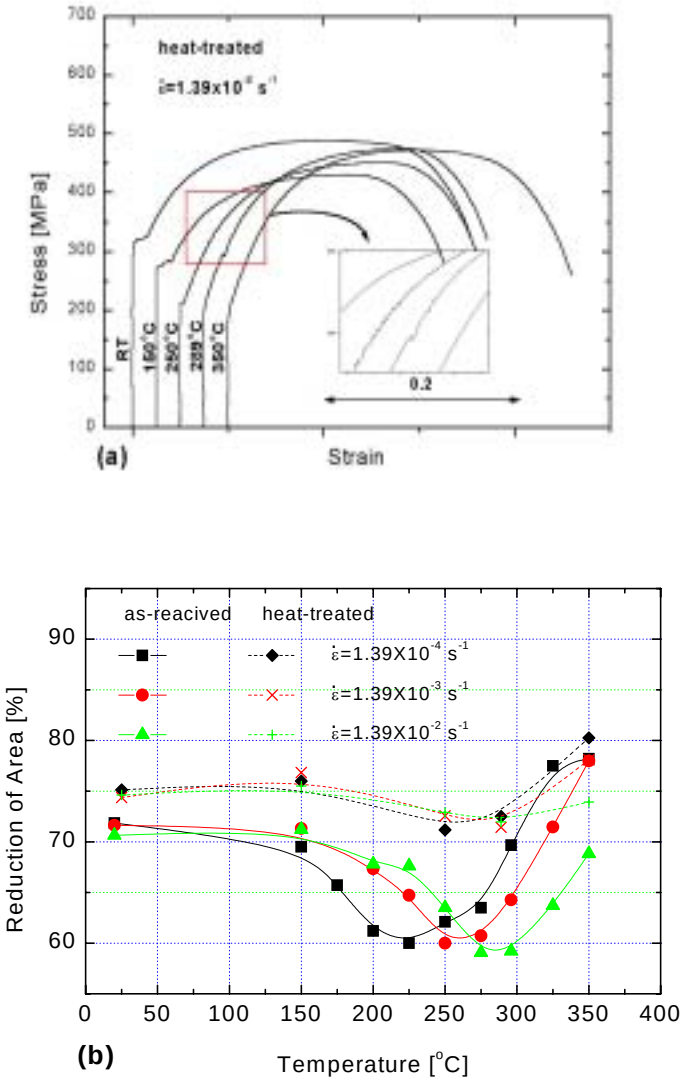

Fig. 3. (a) Stress-strain curves at various temperatures at a strain rate of 1.39×10^{-3} s^{-1}, (b) Comparison of reduction of area between as received [2] and heat-treated specimens.

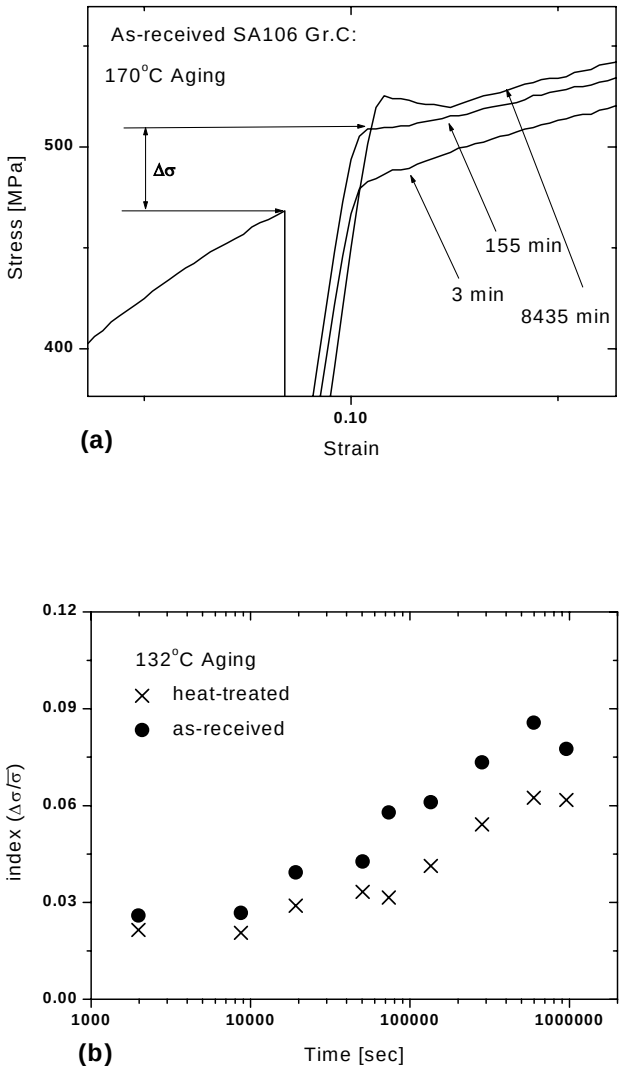

Fig. 4. (a) typical stress-strain curve showing strain aging, (b) aging index increment, $\Delta\sigma/\overline{\sigma}$ *vs* log. aging time for 132°C aging

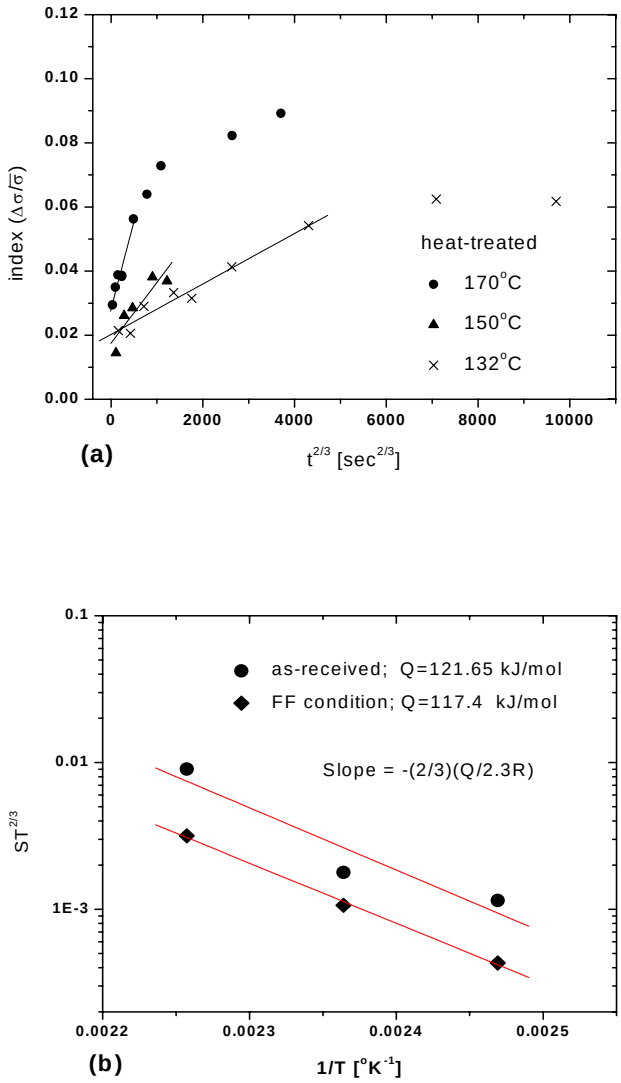

Fig. 5. (a) plot of $\Delta\sigma/\overline{\sigma}$ versus $t^{2/3}$ for heat treated specimen, (b) determination of activation energies of initial stage strain aging both as received and heat-treated.

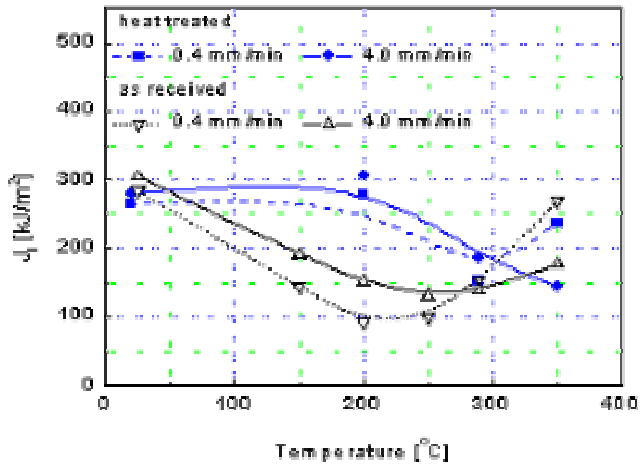

(a)

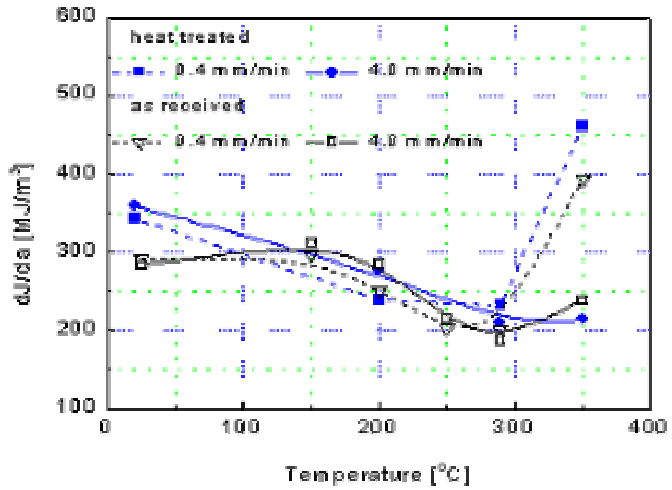

(b)

Fig, 6. Variation in crack initiation fracture toughness, Ji, and crack growth resistance, dJ/da, with temperature at load line displacement rates of 0.4 and 4.0 mm/min.